Optimizing the Synthetic Potential of O_2: Implications of Overpotential in Homogeneous Aerobic Oxidation Catalysis

Alexios G. Stamoulis, David L. Bruns, Shannon S. Stahl*

Department of Chemistry, University of Wisconsin-Madison, Madison, WI 53706 (USA).

Overpotential, aerobic oxidation, catalysis, electrocatalysis, synthesis

ABSTRACT: Molecular oxygen is the quintessential oxidant for organic chemical synthesis, but many challenges continue to limit its utility and breadth of applications. Extensive historical research has focused on overcoming kinetic challenges presented by the ground-state-triplet electronic structure of O_2 and the various reactivity and selectivity challenges associated with reactive oxygen species derived from O_2 reduction. This Perspective will analyze thermodynamic principles underlying catalytic aerobic oxidation reactions, borrowing concepts from the study of the oxygen reduction reaction (ORR) in fuel cells. This analysis is especially important for "oxidase"-type liquid-phase catalytic aerobic oxidation reactions, which proceed by a mechanism that couples two sequential redox half-reactions: (1) substrate oxidation, and (2) oxygen reduction, typically affording H_2O_2 or H_2O. The catalysts for these reactions feature redox potentials that lie between the potentials associated with the substrate oxidation and oxygen reduction reactions, and changes in the catalyst potential lead to variations in effective overpotentials for the two half reactions. Catalysts that operate at low ORR overpotential retain more thermodynamic driving force for the substrate oxidation step, enabling O_2 to be used in more challenging oxidations. While catalysts that operate at high ORR overpotential have less driving force available for substrate oxidation, they often exhibit different or improved chemoselectivity relative to the high-potential catalysts. The concepts are elaborated in a series of case studies to highlight their implications for chemical synthesis. Examples include comparisons of (a) NO_x/oxoammonium and Cu/nitroxyl catalysts, (b) high-potential quinones and amine oxidase biomimetic quinones, and (c) Pd aerobic oxidation catalysts, with or without NO_x cocatalysts. In addition, we show how reductive activation of O_2 provides a means to access potentials not accessible with conventional oxidase-type mechanisms. Overall, this analysis highlights the central role of catalyst overpotential in guiding the development of aerobic oxidation reactions.

Introduction

Molecular oxygen (O_2) is the most abundant and least expensive chemical oxidant available, typically generating water as an environmentally benign byproduct. It is widely used in commodity-scale processes where it is often the only economically and environmentally viable oxidant available.[1–4] Nonetheless, use of O_2 as a synthetically useful oxidant remains one of most daunting fundamental and practical challenges in the fields of chemical synthesis and catalysis. Our research group has been captivated by this topic for over two decades,[5] and has sought to understand mechanistic principles that could broaden the utility of aerobic oxidation reactions. Like others in the field, much of our effort has focused on the design and understanding of catalysts capable of addressing the kinetic challenges encountered in O_2 activation and reduction.[6] More recently, however, our research efforts focused on electrocatalytic oxygen reduction reaction (ORR) have illuminated thermodynamic considerations relevant to synthetic aerobic oxidation reactions. The present Perspective seeks to show how understanding the thermodynamic efficiency of O_2 reduction has important implications for controlling catalytic activity, reactivity, and selectivity in liquid-phase aerobic oxidations of organic molecules.

Several prominent mechanisms have been established for O_2 activation and reactivity with organic molecules. Numerous large-scale industrial processes proceed through radical-chain autoxidation pathways involving well-established initiation, propagation, and termination steps (Figure 1A). Many of these reactions benefit from homogeneous catalysts that control the fate of the reactive intermediates and product selectivity, for example, converting hydroperoxide intermediates into carboxylic acids. Perhaps the most prominent example is the Amoco or Mid-Century process, which uses a Co-Mn-Br cocatalyst system to achieve selective oxidation of xylene to terephthalic acid. Despite their utility, autoxidation methods inherently feature substrates that undergo controlled radical chemistry and lead to oxygenated products.

Other catalytic methods exist for aerobic oxidation of organic molecules that do not proceed via a radical chain pathway. Many of these may be classified as "oxygenase" and "oxidase" reactions, reflecting mechanisms associated with enzymes that catalyze aerobic oxidation. Oxygenases transfer oxygen atoms from O_2 to the substrate, prominent examples of which include cytochrome P450 (Figure 1B) and methane monooxygenase. These enzymes typically require a sacrificial reductant to generate a metal-oxo or other reactive oxygen species responsible for substrate oxidation. Oxidases couple O_2 reduction to substrate oxidation, without oxygen-atom transfer, and they often proceed by a "ping-pong" mechanism that pairs the independent half-reactions (Figure 1C). The oxidase

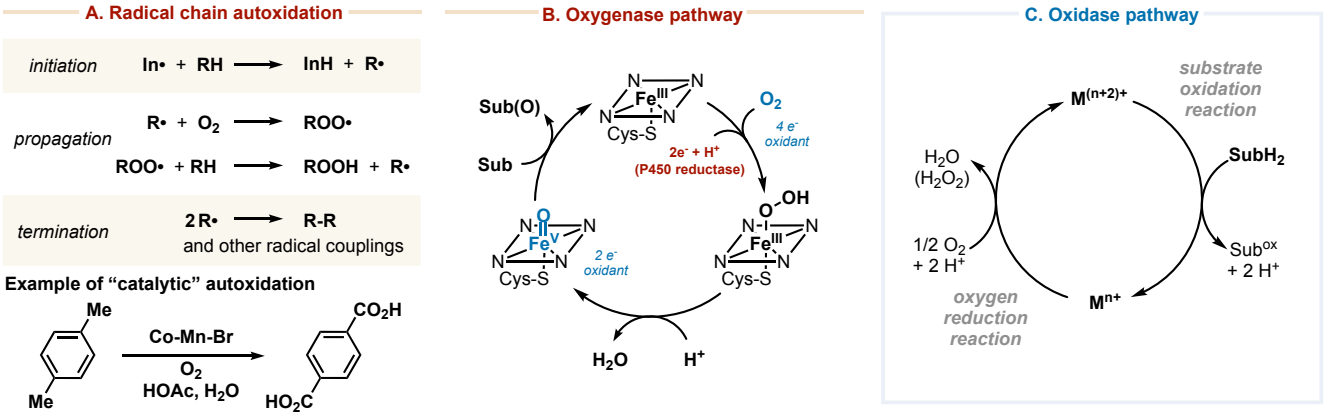

Figure 1. Different classes of aerobic oxidation methods, including (A) radical chain autoxidation, highlighted by the Mid-Century Co-Mn-Br cocatalyzed oxidation of *p*-xylene to terephthalic acid, (B) monooxygenase reactions that feature reductive activation of O_2 to achieve oxygen-atom transfer to organic molecules, exemplified by cytochrome P450 enzymes, and (C) oxidase reactions that couple O_2 reduction and substrate oxidation redox half-reactions.

mechanism provides an appealing platform for development of new aerobic oxidation catalysts because these methods do not need a sacrificial reductant and are formally compatible with any oxidative transformation, including dehydrogenation and dehydrogenative C–O, C–N, and C–C coupling reactions.

Oxidase-type reactions rely on catalyst systems that can promote both of the independent half-reactions in a kinetically efficient manner. This pairing of half-reactions mirrors the electrochemical processes in a fuel cell, where O_2 reduction at the cathode is coupled to H_2 oxidation at the anode; however, there are also differences between these systems. The two half-reactions in a fuel cell take place at two spatially separated electrodes. The difference between the operating electrode potentials (E_{cell}) provides the basis for electricity generation (Figure 2A). In oxidase reactions, an enzyme active site or molecular catalyst mediates both half-reactions. The driving force for each step is defined by the difference between the redox potentials of (a) O_2 and the catalyst and (b) the catalyst and the substrate (Figure 2B).

The thermodynamic efficiency of a fuel cell is strongly affected by the "overpotential" needed to overcome the kinetic barriers for 4 H^+/4 e^- reduction of O_2 to water (η_{ORR}; Figure 2A, red). The overpotential corresponds to the difference between the thermodynamic potential of the chemical reaction (in this case, $E°_{O2/H2O}$ = 1.23 V) and applied potential at the electrode. No current is observed if the cathode is positioned at the thermodynamic ORR potential, but lowering the cathode potential increases the driving force and promotes O_2 reduction. Even the best catalysts require significant overpotential to achieve fast rates. For example, state-of-the-art Pt catalysts exhibit an onset potential of ~0.9 V vs NHE, and even lower potentials are needed to achieve practical current densities (i.e., faster rates).[7] Kinetic barriers and overpotentials for the H_2 oxidation reaction (η_{HOR}; Figure 2A, blue) are much smaller than those encountered with the ORR, hence the smaller value for E_{HOR} in Figure 2A. Higher fuel cell efficiency is achieved by reducing the two overpotentials, η_{ORR} and η_{HOR}.

In this Perspective, we seek to show how the concept of overpotential provides a valuable framework for analyzing oxidase-type aerobic oxidation reactions. As a starting point, there are two relevant overpotential values to be defined. The first corresponds to the effective ORR overpotential arising from the difference between the thermodynamic ORR potential and the catalyst redox potential (η_{ORR}; Figure 2B, red).[8,9] The latter value is analogous to the cathode potential in a fuel cell. The second corresponds to the substrate oxidation overpotential reflecting the difference between the catalyst potential and the thermodynamic potential for substrate oxidation (η_{sub}; Figure 2B, blue). These values are analogous to the anode and HOR potentials in a fuel cell, respectively. As reflected by the energy diagram in Figure 2B, the overpotential for the two half-reactions will be dictated by the redox potential of the catalyst: higher potential catalysts will exhibit lower η_{ORR} and have more thermodynamic driving force available for substrate oxidation, while lower potential catalysts will have lower η_{sub}. This pairing of redox steps means that molecular oxygen can effectively serve as a strong or weak oxidant, with respect to the substrate, depending on the identity of the catalyst.

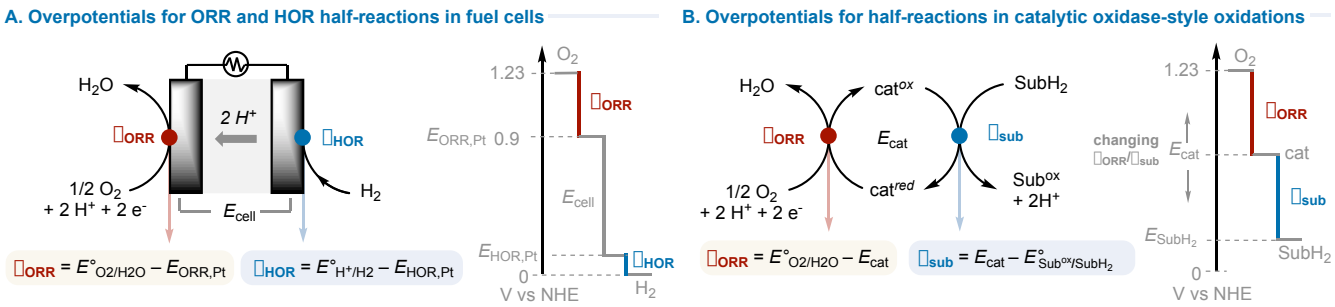

Figure 2. Comparison of redox half-reactions and their overpotentials (η) for (A) an H_2/O_2 fuel cell with Pt-based electrocatalysts for the oxygen reduction and hydrogen oxidation reactions (ORR and HOR, respectively) and (B) homogeneous catalytic aerobic oxidation reactions that proceed via an oxidase-type mechanism.

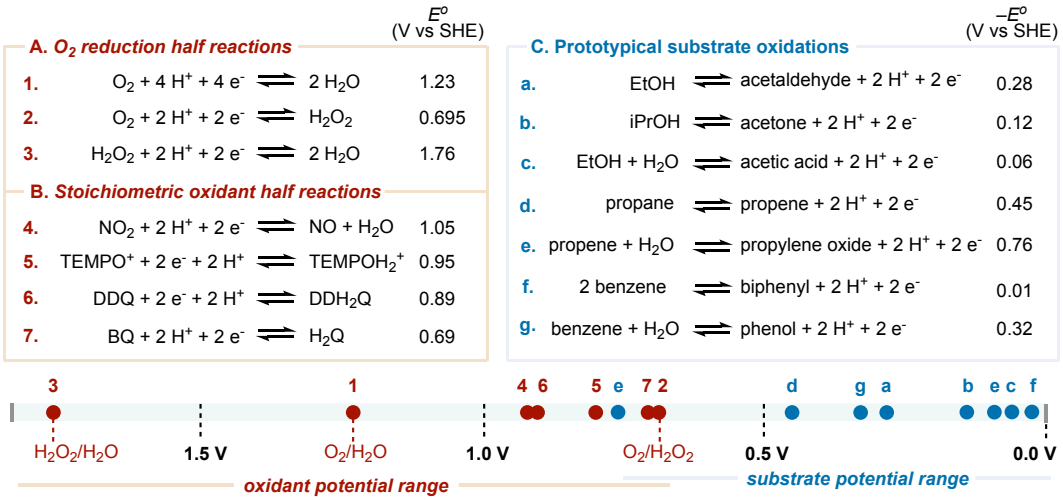

Figure 3. (A) Half-reactions related to oxygen reduction, (B) half-reactions of common oxidants used in organic oxidation reactions, and (C) common organic oxidation reactions as redox half-reactions, all presented with their reduction potentials vs SHE. The difference between the red and blue redox potentials reflects the driving force available for the organic oxidation reactions with the different oxidants (see ref. 11 for additional details and discussion, including derivation of the organic redox potentials).

To conclude this preliminary discussion, we consider redox potentials associated with oxidants and organic substrates pertinent to this analysis (Figure 3). Three important redox potentials associated with molecular oxygen include 4 H^+/4 e^- reduction of O_2 to H_2O (1.23 V), 2 H^+/2 e^- reduction of O_2 to H_2O_2 (0.695 V) and H_2O_2 reduction to H_2O (1.76 V) (Figure 3A).[10] Redox potentials associated with other oxidants and organic substrate oxidations considered in the discussion below are summarized in Figures 3B and 3C, respectively.[11] The O_2/H_2O potential provides adequate thermodynamic driving force to promote all the organic oxidation reactions in Figure 3C. Most of the organic reactions have thermodynamic potentials < 0.5 V. An exception is alkene epoxidation ($E°$ = 0.76 V), but even this reaction has a thermodynamic potential well below the O_2/H_2O potential of 1.23 V.

In the discussion below, we outline four different classes of reactions, which employ catalysts that operate at different overpotentials with respect to O_2 and the organic substrate. We show how variations of the overpotentials in oxidase-type reactions influences their outcomes, including their chemoselectivity, substrate scope, and product identity. We further show how use of a sacrificial reductant has been used in homogeneous catalytic systems to access a higher-potential oxidant to support more-challenging oxidation reactions that are not yet accessible via a conventional oxidase mechanism.

Note on (Over)Potential Values. The potential values discussed herein are obtained from the literature or derived from thermochemical data (see reference 11 for a discussion of the derivations). These values will be used in a semi-quantitative way, recognizing that the precise values will depend on the reaction conditions, for example, the pH of an aqueous solution or the identity of an organic solvent. Nonetheless, because the half-reactions for both oxidants and organic substrates involve transfer of an equal number of protons and electrons, the relative redox potentials should remain constant. Even relatively large deviations from this assumption (e.g., 100-200 mV) will not alter the conclusions drawn from the analysis outlined below.

We separately note that many oxidase-type aerobic oxidation reactions employ cocatalysts or mediators (first presented in Figure 4A below). This feature introduces some ambiguity into the definition of the ORR overpotential, as η_{ORR} could be defined with respect to the initial reaction of O_2 with the catalyst/cocatalyst/mediator, or with respect to the catalyst that mediates substrate oxidation. The graphics below (e.g., Figure 4A) illustrate the former, since the initial step formally corresponds to the ORR. The latter approach is also viable, however, because it conveys the net loss in driving force from O_2 reduction that remains available to promote substrate oxidation. In short, both approaches are relevant to the analysis herein, and the potential ambiguity is acknowledged.

Nitroxyl-catalyzed oxidations: Oxoammonium versus Cu/nitroxyl catalysts.

Oxoammonium-based oxidants are widely used in organic synthesis for diverse transformations,[12,13] including alcohol[14–18] and amine[19–21] oxidation, oxidative cleavage of ethers,[22,23] and C–H oxidation reactions (Figure 4A).[24,25] Though they are often employed as stoichiometric oxidants, many catalytic variants have been developed using terminal oxidants such as NaOCl,[26] oxone,[27] and hypervalent iodine,[28] or using electrochemistry.[13] Oxoammonium-mediated alcohol oxidation can proceed by two different mechanisms, depending on the pH of the reaction mixture: under acidic conditions, the reaction involves bimolecular hydride transfer from the alcohol to the oxoammonium (Figure 4A), while basic conditions lead to formation of an alkoxide/oxoammonium adduct that undergoes intramolecular hydride transfer.[15]

2,2,6,6-Tetramethyl-1-oxo-piperidinium ($TEMPO^+$) is the prototypical example of an oxoammonium oxidant and has a standard potential of 0.95 V vs SHE for the 2 H^+/2 e^- reduction to $TEMPOH_2^+$.[12,29] The high potential values of oxoammonium reagents have two important consequences for their synthetic and catalytic applications. First, oxoammonium reagents have inherently small η_{ORR} values since the oxoammonium potential lies close to the O_2/H_2O potential. Consequently, regeneration of $TEMPO^+$ from TEMPOH generally requires the use of a strong chemical oxidant, such as NaOCl or $PhI(OAc)_2$. Kinetic limitations make the regeneration of $TEMPO^+$ from TEMPOH (or $TEMPOH_2^+$, under acidic conditions) with O_2 challenging, and a direct autoxidation process is not practically feasible.

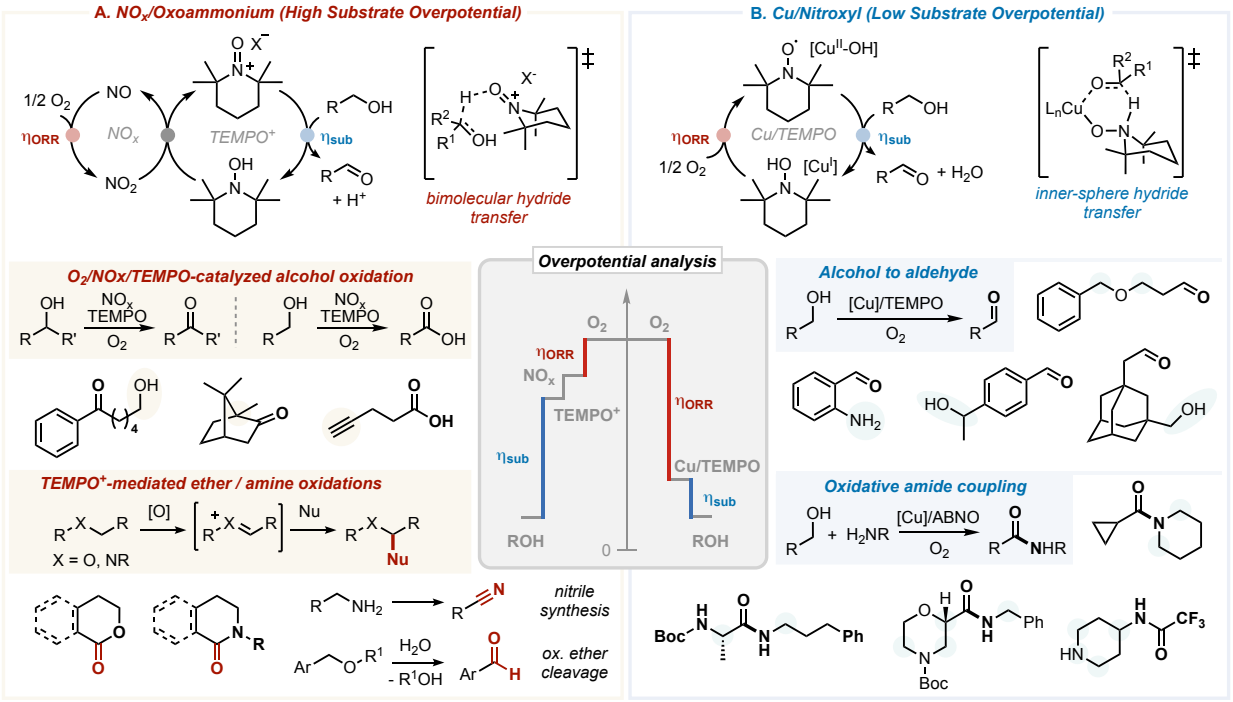

Figure 4. Comparison of (A) NO_x/oxoammonium-catalyzed aerobic oxidation of organic molecules and (B) Cu/TEMPO-catalyzed alcohol oxidation reactions. Cu/TEMPO features a mechanism in which Cu^{II} and TEMPO serve as cooperative one-electron oxidants, avoiding formation of the high-potential oxoammonium species. This mechanistic difference results in a lower overpotential for substrate oxidation (η_{sub}) and rationalizes the high chemoselectivity for alcohol oxidation in the presence of other oxidatively sensitive functional groups.

Nonetheless, the NO_2/NO 2 H^+/2 e^- standard potential is 1.05 V and NO undergoes efficient reaction with O_2 to generate NO_2. This reactivity provides the basis for NO_x-based cocatalysts in TEMPO-catalyzed aerobic oxidation of organic molecules (Figure 4A). On the basis of standard reduction potentials, O_2 reduction at the NO_2/NO potential means that only 0.18 V of driving force is lost in the redox cascade from O_2 to NO_2, and NO_2 promotes efficient oxidation of TEMPO and TEMPOH to $TEMPO^+$ with only 100 mV driving force (1.05 V – 0.95 V).

We have independently used electrochemical studies to evaluate the thermodynamic efficiency of O_2 reduction with a NO_x/TEMPO cocatalyst system in acetonitrile (i.e., under non-standard-state conditions).[30] These studies revealed that ORR proceeds with an effective overpotential of only 300 mV, closely matching that predicted from the standard-state analysis and demonstrating that this system rivals the low overpotentials observed with state-of-the-art Pt ORR catalysts in fuel cells.

The high reduction potentials of oxoammonium reagents mean that they are good oxidants for organic substrates. According to the analysis in Figure 2B, their high potential corresponds to a large overpotential for substrate oxidation, η_{sub}. For instance, the η_{sub} values for the oxidation of ethanol (1° alcohol) to acetaldehyde, and isopropanol (2° alcohol) to acetone with $TEMPO^+$ are 0.67 V and 0.83 V, respectively. These large values make relatively high-energy hydride-transfer mechanisms possible and account for the diverse reactivity depicted in Figure 4A).[31,32] Another consequence of the large driving force, however, is relatively limited chemoselectivity that can lead to poor discrimination between alcohols and other functional groups that can undergo hydride or electron transfer. The aerobic NO_x-based cocatalyst systems, which feature reactive NO_2 and NO radicals, further limit the scope and functional group compatibility of oxoammonium-based oxidation methods due to the incompatibility of NO_x species with oxidatively sensitive functionalities, such as amines.

Cu/nitroxyl catalyst systems also feature TEMPO or another nitroxyl cocatalyst, but these aerobic oxidation reactions often show exquisite selectivity for alcohol oxidation in the presence of other oxidatively sensitive functional groups, such as amines and activated C–H bonds (Figure 4B).[33] Mechanistic studies of alcohol oxidation with (bpy)Cu/nitroxyl catalysts (bpy = 2,2'-bipyridine) implicate the formation of a (bpy)Cu(alkoxide)(nitroxyl) intermediate. Net hydride transfer occurs from this intermediate through a six-membered transition-state structure, shown in Figure 4B, to generate the carbonyl product, $(bpy)Cu^I$, and TEMPOH.[34–36] The oxidized $(bpy)Cu^{II}$ and TEMPO species are then regenerated by O_2.

Comparison of the oxoammonium and Cu/nitroxyl-mediated oxidation reactions highlights a key mechanistic difference: the Cu/TEMPO-catalyzed alcohol oxidation reactions do not involve the high-potential oxoammonium species. Cu^{II} and TEMPO serve as cooperative one-electron oxidants in the two-electron hydride-transfer step. This mechanistic difference, which manifests itself in different overpotentials for the two half-reactions (η_{ORR} and η_{sub}), rationalizes the high chemoselectivity observed for Cu/nitroxyl-catalyzed alcohol oxidation. Electrochemical studies show that the Cu/nitroxyl catalyst promotes alcohol oxidation at the $Cu^{II/I}$ potential, which is 0.4–0.5 V below the TEMPO/$TEMPO^+$ potential.[37,38] Briefly, by operating with a relatively large overpotential for O_2 reduction, the Cu/TEMPO catalyst system serves as a mild oxidant that operates with a comparatively low overpotential for alcohol oxidation, which allows it to tolerate other oxidatively sensitive functional groups. Kinetic analysis has further shown that, in spite of the significantly lower driving force for alcohol

oxidation, Cu/TEMPO exhibits turnover frequencies 4-5-fold higher than TEMPO$^+$.[37] This inverted overpotential/rate correlation suggests the cooperative Cu/TEMPO mechanism is especially well tuned for alcohol oxidation. An important implication of this study is that catalysts that operate efficiently with a low η_{sub} increase prospects to achieve high chemoselectivity.

Quinone-catalyzed oxidations: DDQ versus amine oxidase mimics

The effect of η_{ORR} and η_{sub} on chemoselectivity is also evident in quinone-mediated oxidations. Like nitroxyl-based oxidants, quinones have widespread utility in chemical synthesis.[39] 2,3-Dichloro-5,6-dicyano-p-benzoquinone (DDQ) is a prominent high-potential quinone that has a 2 H^+/2 e^- standard reduction potential of 0.89 V vs RHE.[40] DDQ is used in a wide range of organic oxidation reactions, including alcohol and amine oxidations, oxidative deprotection of alcohols, dehydrogenation of saturated heterocycles, and oxidative C–C coupling.[39] The high DDQ/$DDQH_2$ redox potential provides the driving force to promote direct electron- and hydride-transfer from diverse organic molecules,[41,42] but this feature makes it difficult to use DDQ as a catalyst, owing the difficulty in oxidizing $DDQH_2$. DDQ is typically used as a stoichiometric reagent; however, NO_x-based cocatalysts support aerobic oxidation of $DDQH_2$ and provide the basis for DDQ-catalyzed aerobic oxidation of organic molecules (Figure 5A).

DDQ exhibits a high overpotential (η_{sub}) for organic oxidation reactions that can create chemoselectivity challenges with substrates that have multiple oxidatively sensitive functional groups. The reactivity and properties of DDQ may be compared to a different family of quinones that resemble the active-site cofactor in Cu-amine oxidases and promote the oxidative dehydrogenation of amines.[39,43–46] Different mechanisms are possible for these reactions, but studies generally support formation of a covalent adduct between the amine and the quinone, either as an imine or hemiaminal, followed by electrocyclic hydride transfer. Various synthetic quinones, including 4-tert-butyl-2-hydroxybenzoquinone (TBHBQ),[47] (phd)ZnX_2 (phd = 1,10-phenanthroline-5,6-dione),[48] and $[Ru(phd)_3]^{2+}$,[49,50] have been used to support aerobic oxidative dehydrogenation of 1°, 2°, and 3° amines.

The dehydrogenation of 3° indolines using a $[Ru(phd)_3]^{2+}$/Co(salophen) cocatalyst system (Figure 5B)[50] is particularly relevant to the present discussion because this chemical reaction is commonly achieved with stoichiometric DDQ.[51] Mechanistic data suggest $[Ru(phd)_3]^{2+}$ promotes this reaction via adduct formation and electrocyclic hydride transfer, and the Co(salophen) cocatalyst is proposed to mediate hydroquinone reoxidation by O_2. The distinction between this catalyst system and DDQ is evident from a comparison of their respective functional group compatibility, evaluated by testing the dehydrogenation of 5-bromo-1-methylindoline in the presence of oxidatively sensitive molecules, including diphenylmethane, dihydrobenzofuran, dihydrobenzopyran, an allylic alcohol, a 3° lactam, and *N*-Boc-pyrrolidine (Figure 5B).[50] The $[Ru(phd)_3]^{2+}$ catalyst system retained excellent yield of the indole in all cases and near-quantitative recovery of the additive. In contrast, DDQ led to significantly reduced yield of the indole and significant consumption of the additive.

These results may be rationalized by analyzing the relative overpotentials of the two systems. Aerobic oxidation reactions employing the DDQ/NO_x/O_2 catalyst system feature a relatively low η_{ORR}, stepping down from 1.23 V (O_2/H_2O) to 1.05 V

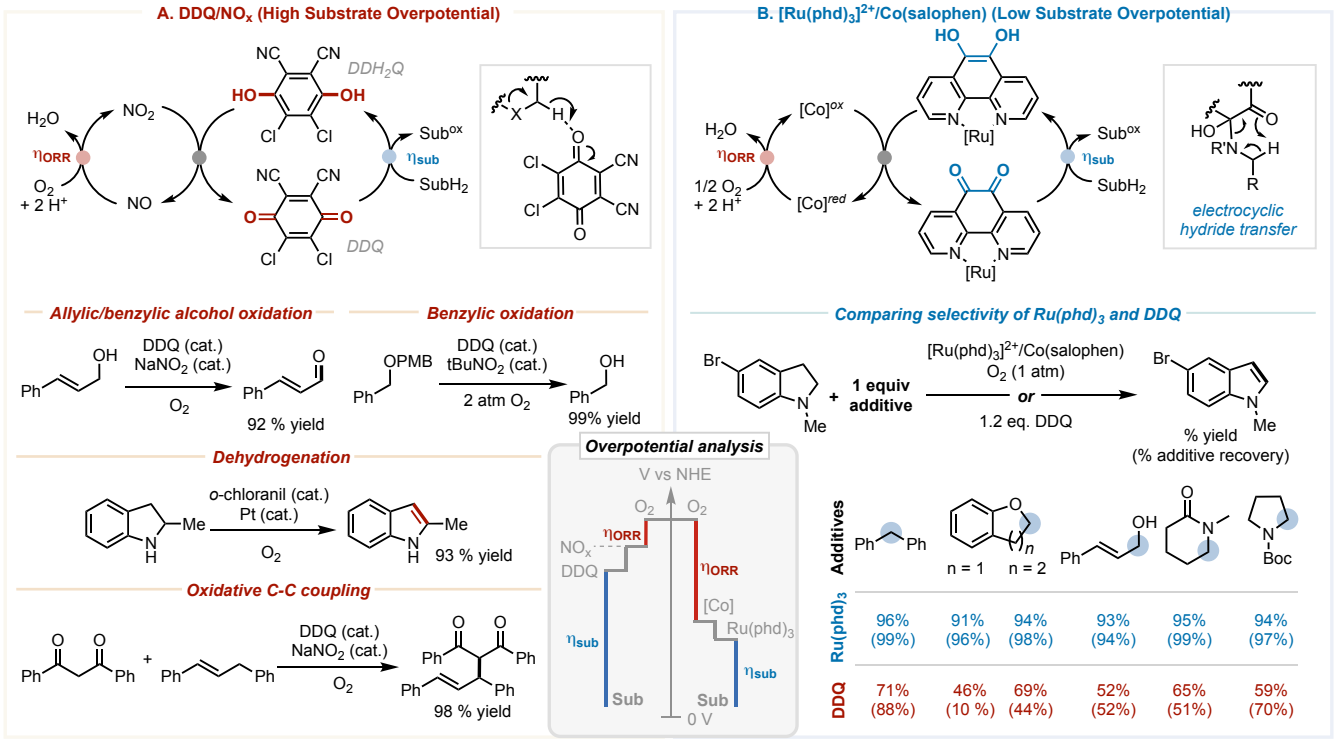

Figure 5. Comparison of (A) DDQ/NO_x-catalyzed oxidation of organic molecules and (B) $[Ru(phd)_3]^{2+}$/Co(salophen)-catalyzed aerobic dehydrogenation of amines (including 1°, 2°, and 3° amines). DDQ is a much stronger oxidant (high η_{sub}) than $[Ru(phd)_3]^{2+}$ and shows a broader scope of reactivity, while $[Ru(phd)_3]^{2+}$ has a lower η_{sub} and mediates highly chemoselective dehydrogenation of amines and tolerates diverse oxidatively sensitive functional groups.

(NO_2/NO) to 0.89 V (DDQ/$DDQH_2$). On the other hand, Co(N_2O_2) complexes, including Co(salophen), have been studied as molecular electrocatalysts for ORR, and they generate H_2O_2 as the initial product.[52] Although ORR product selectivity and the precise redox potential can vary with the reaction conditions, these observations implicate a relatively large η_{ORR} (Figure 5, right side of the Overpotential Analysis inset). The 2 H^+/2 e^- reduction potential of $[Ru(phd)_3]^{2+}$ has not been reported; however, the one-electron reduction potential of $[Ru(phd)_3]^{2+}$ is 0.73 V lower than DDQ under identical conditions ($E_{1/2}$ = –0.59 V vs 0.14 V, respectively, vs $Fc^{+/0}$).[50] These data reveal that the $[Ru(phd)_3]^{2+}$ catalyst operates with a much lower overpotential for substrate oxidation (i.e., η_{sub}) relative to DDQ.

Collectively, these considerations resemble the comparison of oxoammonium and Cu/nitroxyl catalyst system. In both cases, a NO_x-based cocatalyst system allows O_2 to be used as terminal oxidant with a high-potential reagent (oxoammonium or DDQ). This reactivity is made possible by the low η_{ORR} for NO_x-mediated ORR. On the other hand, the Cu/nitroxyl and $[Ru(phd)_3]^{2+}$/Co(salophen) catalyst systems operate at lower potential, reflecting higher η_{ORR} but lower η_{sub}. This feature enables these catalysts to mediate aerobic oxidation of alcohols and amines, respectively, with high chemoselectivity and broad tolerance of other oxidatively sensitive functional groups.

Pd-catalyzed aerobic oxidations: Tuning overpotential to access different products.

Palladium-catalyzed oxidation reactions are widely used in organic chemistry to achieve dehydrogenation and dehydrogenative coupling of organic molecules. The majority of these reactions proceed via an oxidase-type mechanism with two half reactions: substrate oxidation by Pd^{II} and reoxidation of Pd^0 by an oxidant, such as O_2, benzoquinone (BQ), and Cu^{II} and Ag^I salts.[53–58] A complementary class of reactions features a $Pd^{II/IV}$ cycle, in which a strong oxidant such as $PhI(OAc)_2$, peroxides, or another reagent intercepts an organopalladium(II) intermediate to generate a Pd^{IV} species that undergoes more facile reductive elimination.[59–63] The $Pd^{II/0}$ and $Pd^{II/IV}$ reaction classes support different reactions, and both are now commonly used in organic synthesis. Pd-catalyzed oxidative coupling of benzene to biphenyl and phenyl acetate[64] are prototypical examples of these reaction classes and provide excellent case studies for the consideration of overpotential.

The oxidative coupling of benzene to biphenyl and the oxygenation of benzene to phenol have significantly different standard potentials: 0.01 V and 0.32 V, respectively, vs SHE (Figure 3C, entries f and g; phenol is used as a surrogate for PhOAc[65]). Despite the >300 mV difference, both values are well below the thermodynamic potential for O_2 reduction to H_2O (1.23 V). But, the oxidation of Pd^0 by O_2 typically generates H_2O_2 as an initial product,[66-68] indicating that O_2 reduction to H_2O_2 is the relevant ORR potential (0.695 V) for reactions involving a $Pd^{II/0}$ cycle. Reactions of Pd^{II} complexes with O_2 are exceedingly rare, with a prominent exception reported by Mirica and coworkers, who used a tetradentate ligand to promote the oxidation of a dimethyl-Pd^{II} species to Pd^{IV} with O_2 via an intermediate superoxide adduct.[69] Consideration of the Pd/O_2 reactivity associated with the ORR step is complemented by assessment of Pd-based redox potentials that establish the overpotentials for both half-reactions. $Pd^{II/0}$ and $Pd^{II/IV}$ redox steps for catalytically relevant Pd complexes are generally not well-behaved electrochemically because significant changes take place in the Pd coordination environment upon oxidation and reduction. Nonetheless, we recently established $Pd^{II/0}$ redox equilibria with BQ/BQH_2 that

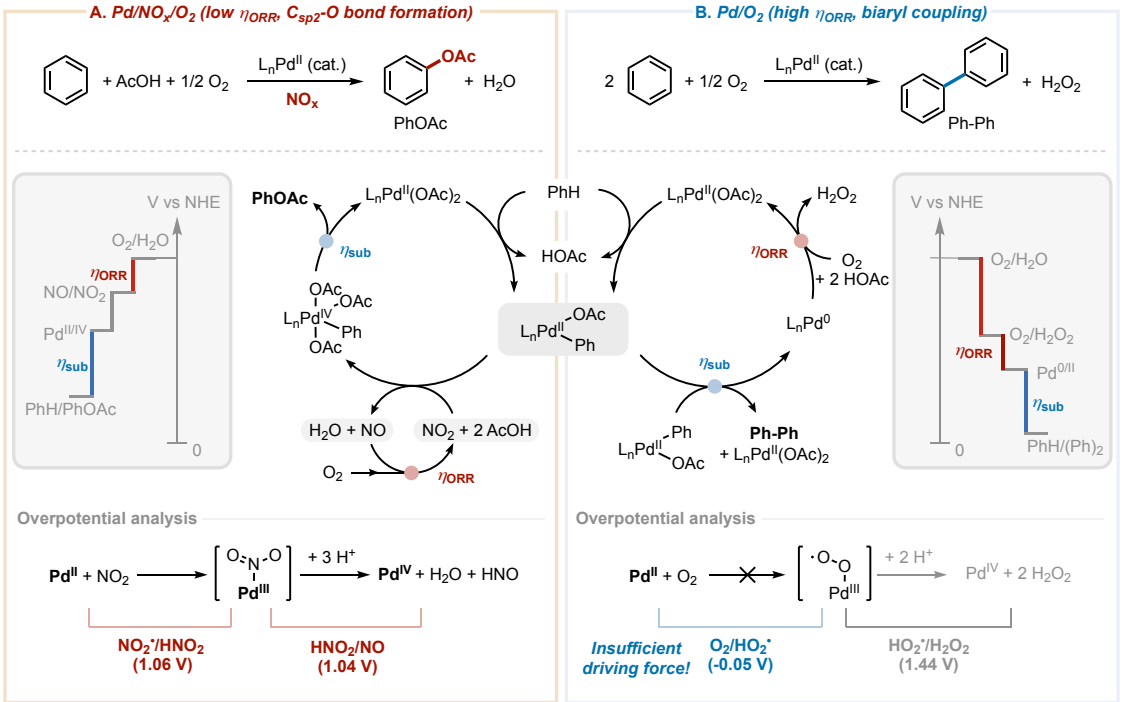

Figure 6. Comparison of aerobic (A) Pd/NO_x-catalyzed acetoxylation of benzene and (B) Pd-catalyzed biaryl coupling. Both pathways share a common $L_nPd^{II}(OAc)(Ph)$ intermediate, but the low η_{ORR} NO_x cocatalyst supports oxidation of Pd^{II} to Pd^{IV} (lower left inset) to enable C–O reductive elimination. In the absence of NO_x, the O_2 is kinetically inert toward Pd^{II} (the $O_2/HO_2^{\bullet}$ redox potential is too low; lower right inset) and, therefore, transmetalation between two $L_nPd^{II}(OAc)(Ph)$ species affords a $L_nPd(Ph)_2$ species (not shown) that undergoes C–C reductive elimination to yield biphenyl.

provided reliable values for $Pd^{II/0}$ redox potentials.[70] $Pd^{II}(OAc)_2$ with various nitrogen-based ligands (e.g., pyridine, bpy, and phenanthroline derivatives) exhibit redox potentials of approximately 350-650 mV vs SHE, based on experimental and computational analysis of their equilibria with BQ/BQH_2 derivatives. Although these values will depend on specific reaction conditions, this range of values suggests that Pd^{II} may not be a strong enough oxidant to promote oxidative coupling of benzene to phenyl acetate. The lack of suitable experimental $Pd^{II/0}$ and $Pd^{II/IV}$ redox potentials limits more thorough assessment of this issue; however, catalytic studies of oxidative coupling provide clear insights into role of overpotential in Pd-catalyzed aerobic oxidation reactions.

Pd-catalyzed oxidative coupling of benzene to biphenyl is initiated by C–H activation of Ph–H by the $L_nPd(OAc)_2$ catalyst to generate $L_nPd(OAc)(Ph)$ (Figure 6B).[54,71] A recent mechanistic study showed that biaryl homocoupling proceeds via transmetalation between two $L_nPd(OAc)(Ar)$ species to form a $L_nPd(Ar)_2$ intermediate.[72] This intermediate can undergo C–C reductive elimination to afford biaryl and Pd^0, which can undergo oxidation by O_2. As noted above, the formation of H_2O_2 in the Pd^0 oxidation step limits the driving force available from O_2, establishing the O_2/H_2O_2 potential as an upper limit (0.695 V vs SHE). This feature, which imposes a rather large η_{ORR} on the reaction, is not necessarily problematic for thermodynamically and kinetically facile reactions, and many examples of $Pd^{II/0}$-catalyzed oxidation reactions exist that use O_2 as a terminal oxidant through a similar reaction pathway.[53-58]

Pd-catalyzed oxidative coupling of benzene to PhOAc is initiated by the same $L_nPd(OAc)_2$-mediated C–H activation step to afford $L_nPd(OAc)(Ph)$. A strong oxidant, such as $PhI(OAc)_2$,[73] can intercept this intermediate before it undergoes transmetalation to generate a high-valent Pd(Ph)(OAc) species, and the latter species undergoes facile reductive elimination to afford PhOAc. There are now many examples of Pd-catalyzed oxidative coupling reactions involving Pd^{III} or Pd^{IV} intermediates.[59–63] While precise redox potentials are not known, the Pd^{III}/Pd^{IV} intermediates are expected to have higher potentials than Pd^{II} species and should thereby facilitate more challenging substrate oxidations.

Relatively few Pd-catalyzed reactions with high-valent Pd intermediates use O_2 as the oxidant. The majority of examples employ NO_x-based cocatalysts,[64,74–80] similar to the high-potential aerobic oxidation reactions involving oxoammonium and quinone catalysts.

The reaction of O_2 with Pd^{II} is initiated by formation of a Pd^{III}-superoxide species;[69] however, O_2 is a very poor one-electron oxidant ($E°_{O2/HO2}$ = -0.05 V). In contrast, NO_2 is a very strong one-electron oxidant ($E°_{NO2/HNO2}$ = 1.06 V). NO_2 is also a strong two-electron oxidant relative to O_2 ($E°_{O2/H2O2}$ = 0.695 V vs $E°_{NO2/NO}$ = 1.05 V). Thus, the introduction of NO_x cocatalysts into Pd-catalyzed aerobic oxidation reactions provides a means to access high-valent organopalladium intermediates and leverage $Pd^{II/IV}$ reaction pathways, rather than the more conventional $Pd^{II/0}$ aerobic oxidation pathways. This feature is exemplified by the Pd-catalyzed oxidative coupling of benzene and acetic acid in the presence of O_2 and fuming HNO_3 (one of several precursors used to generate NO_2/NO in situ) to form phenyl acetate (Figure 6A).

The influence of NO_x cocatalysis can again be analyzed according to the overpotentials associated with the two half-reactions. NO_x cocatalysts support O_2 reduction at low η_{ORR}, thus preserving more of the thermodynamic potential from O_2 to be used for the substrate oxidation half-reaction. The generation of higher oxidation state Pd species increases the η_{sub}, allowing more challenging substrate oxidation reactions to be achieved.

In situ generation of organic peroxides: Accessing higher potential oxidants via reductive activation of O_2

The case studies outlined above show how NO_x cocatalysts generate high-potential catalysts from O_2, taking advantage of the low ORR overpotential available from the NO_2/NO redox couple. Nonetheless, some synthetic oxidation reactions require an oxidant that is even stronger than that accessible from NO_x/O_2. The monooxygenase mechanism depicted in Figure 1B shows how nature addresses this limitation in biological oxidations. A sacrificial reductant, such as NADH, is used by monooxygenases to convert O_2 from a four-electron oxidant with a standard potential of 1.23 V into a two-electron oxidant that leverages the higher redox potential of hydrogen peroxide with a standard potential of 1.76 V ($E°_{H2O2/H2O}$). Metal-oxo intermediates, such as those featured in cytochrome P450, are often generated by protonation/dehydration of a hydroperoxide intermediate, and the same intermediates often may be generated by direct reaction of hydrogen peroxide with Fe^{III} or related catalyst precursors.[81,82] Integrating reductive activation of O_2 into synthetic oxidation reactions is complicated by the requisite inclusion of both an oxidant (O_2) and a reductant into the same reaction mixture; however, several successful examples have been achieved. Some of the most synthetically relevant examples have used aldehydes as the sacrificial reductant (Sac–H), using in situ generation of an acyl peroxide (Figure 7), which represents a high-potential oxidant that supports alkene epoxidation,[83,84] C–H amination,[85] and generation of hypervalent iodine reagents.[86,87]

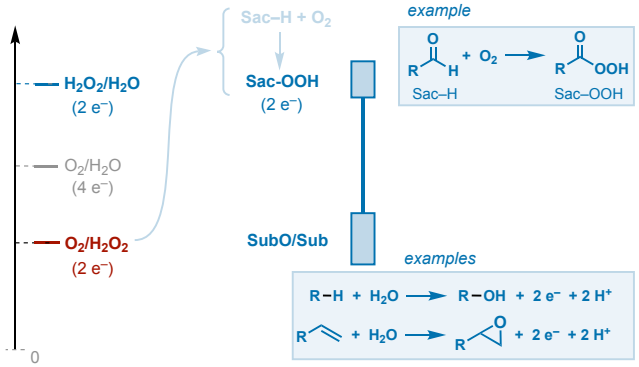

Figure 7. Energy diagrams highlighting the use of a sacrificial reductant (Sac–H), such as an aldehyde, to promote 2 e^- reduction of O_2 to generate a peroxide or other strong oxidant, capable of promoting challenging oxidation reactions, such as C–H oxidation or alkene epoxidation. The precise values of the high-potential oxidants and organic oxidation reactions can vary.

Aldehyde-promoted aerobic epoxidation of alkenes (Mukaiyama Epoxidation). The epoxidation of alkenes is one of the most thermodynamically challenging organic oxidation reactions. For example, the propylene/propylene oxide redox reaction has a standard potential of 0.76 V vs SHE (cf. Figure 3B).[11] Strongly oxidizing reagents such as NaOCl, oxone, and organic peroxides are typically employed in their synthesis, often in the presence of a transition metal catalyst.[88,89]

In the early 1990s, Mukaiyama and coworkers reported Ni-catalyzed epoxidation of substituted alkenes with O_2, using an aldehyde as a sacrificial reductant (Figure 8A),[83,84] and analogous reactivity was reported with Mn and Fe-based catalysts.[90,91] Subsequent mechanistic studies showed that the Ni catalyst initiates aldehyde autoxidation to generate an acylperoxyl radical, which adds to the alkene and then undergoes O-atom transfer from the alkylated peracyl intermediate.[92] A peracid can also form under the reaction conditions and mediate epoxidation of the alkene substrate (Prilezhaev reaction).[92] Other studies show that epoxidation in the absence of a metal cocatalyst can take place via parallel acylperoxyl radical and peracid-mediated epoxidation pathways.[93–95] Conditions can be biased to promote the peracid-mediated epoxidation pathway (e.g. by using excess aldehyde), benefiting from the coarctate transition state to retain the olefin stereochemistry in the epoxide (Figure 8B).[96,97] Mukaiyama epoxidation reactions are prototypical chemical examples of monooxygenase reactivity, wherein reductive activation of O_2 generates a higher-potential oxidant capable of promoting a thermodynamically challenging oxidation reaction.

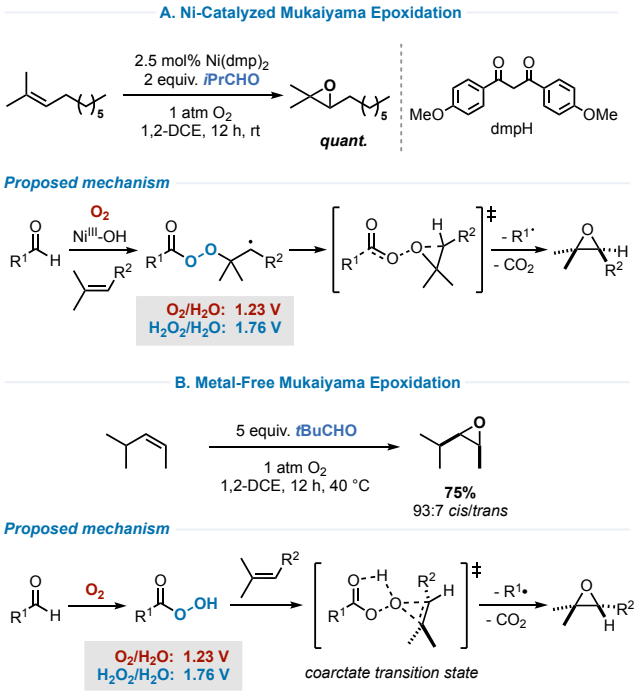

Figure 8. (A) Ni-catalyzed Mukaiyama epoxidation of alkenes, and the proposed mechanism, highlighting in situ generation of an acylperoxyl species as a high-potential oxidant capable of promoting oxygen-atom transfer. (B) Catalyst-free Mukaiyama epoxidation of alkenes, showing the peracid-mediated epoxidation pathway.

Glycolic acid/1,4-dioxane-promoted aerobic Pd-catalyzed aryl C–H amination. Pd-catalyzed aerobic oxidative coupling of C–H bonds with heteroatom nucleophiles is challenging, as discussed above for the coupling of benzene and acetic acid. Similar issues are encountered with C–N coupling reactions. In this context, we serendipitously discovered that autoxidation of glycolic acid and dioxane in situ generates an organic peroxide capable of promoting Pd-catalyzed C–N coupling via a $Pd^{II/IV}$ pathway (Figure 9).[85] The reaction employs (DAF)$Pd(OAc)_2$ (DAF = 4,5-diazafluoren-9-one) as the catalyst and promotes intramolecular oxidative C–H amination of N-benzenesulfonyl-2-aminobiphenyl **1** to afford N-benzenesulfonylcarbazole **2**. Control experiments showed that **2** could be formed in comparable yields through the intentional addition of peroxides such as tert-butylhydroperoxide. The results resemble those from earlier studies showing that autoxidation of tetrahydrofuran (THF) solvent generates a peroxide species in situ that promotes Wacker-type oxidation of alkenes and other reactions.[98,99] Toluene autoxidation has been shown to support the directed hydroxylation of 2-phenylpyridine and related substrates via a $Pd^{II/IV}$ mechanism.[100] These examples show how O_2 may be used in combination with a sacrificial reductant to access peroxides that support Pd-catalyzed oxidation reactions. In many cases, direct use of a peroxide-based oxidant (e.g., *t*BuOOH) will be a more practical approach to conduct these reactions.[101]

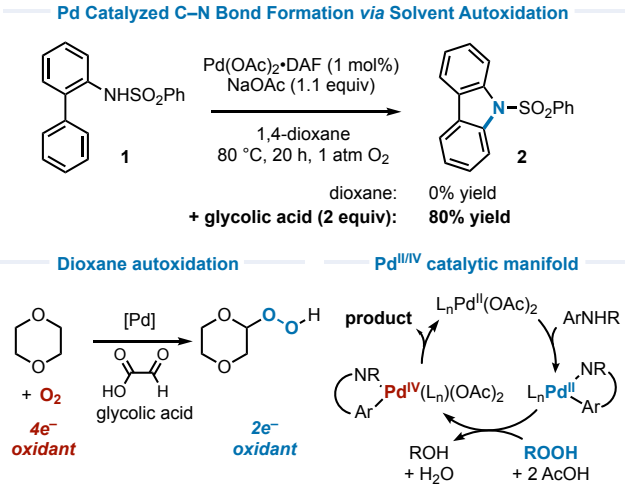

Figure 9. $Pd^{II/IV}$–mediated aerobic intramolecular C-N bond formation enabled by dioxane autoxidation and in situ peroxide formation.

Aldehyde-promoted aerobic generation of hypervalent iodine reagents. Hypervalent iodine reagents are strong oxidants and see widespread use in synthetic chemistry.[102] They are typified by $PhI(OAc)_2$ (0.91 V vs SHE)[103] and are commonly generated by oxidation of iodobenzene with strong oxidants such as persulfate, periodate, and permanganate, with potentials at 2.08, 1.59, and 1.49 V vs SHE, respectively.[11,104] O_2 theoretically has sufficient driving force to generate hypervalent iodine reagents, but effective methods were not reported until recently. Successful reactivity is achieved by leveraging reductive activation of O_2 to access a higher potential oxidant.

Powers and coworkers demonstrated the use of acetaldehyde as a sacrificial reductant to support aerobic oxidation of iodoarenes to various I^{III} reagents, such as $PhI(OAc)_2$ and PhIO (Figure 10).[86,87,105] This in situ generation of hypervalent iodine reagents with O_2 as the stoichiometric oxidant has been applied to a variety of organic oxidation reactions, including oxidative difunctionalization of alkenes, alpha-C–H oxygenation and bromination of ketones, and amidation of arene C–H bonds (Figure 10).

Conclusions

Overpotential is a metric that has been primarily used in the field of electrocatalysis to assess the thermodynamic efficiency of an electrochemical catalyst and/or catalytic reaction. In this Perspective, we show how this metric may be used to evaluate thermal catalyst systems, specifically those used in homogeneous aerobic oxidation reactions. Homogeneous

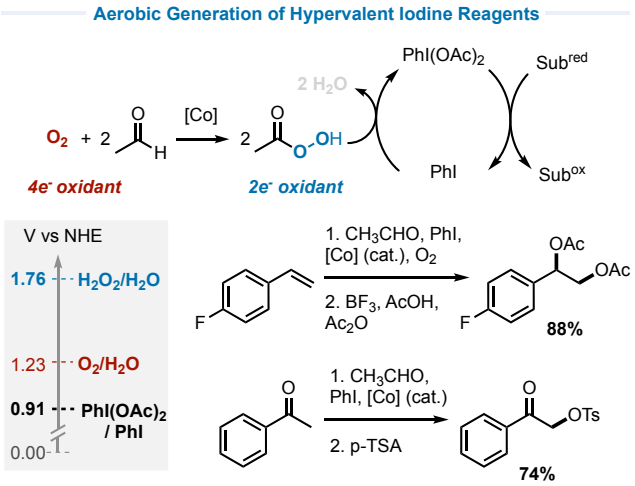

Figure 10. High-potential acyl hydroperoxides may be generated via autoxidation of acetaldehyde as a means to generate iodine(III) reagents with O_2.

catalysts and cocatalyst systems of the type elaborated herein feature redox potentials that lie between the thermodynamic potentials for the O_2 reduction and substrate oxidation half-reactions. The data show that the different overpotentials have implications for reactivity and chemoselectivity, with the latter manifested in different ways, including functional group compatibility and/or product identity. Cocatalysts that activate O_2 at low overpotential, such as NO_x species, enable the aerobic generation of high-potential catalysts, including oxoammonium species, DDQ, and Pd^{IV}, that have widespread utility in organic synthesis. The NO_2 and NO cocatalyst species generated from various NO_x precursors are reactive gases and can be difficult to handle. This consideration provides motivation to develop new cocatalysts that operate at low η_{ORR}. Such reagents could significantly expand the scope of aerobic oxidation reactions. The analysis herein, however, also shows that low η_{ORR} is not always optimal in homogeneous catalytic oxidation reactions. In some cases, it is preferable to have catalysts that operate at high η_{ORR}, with a correspondingly lower η_{sub}. Catalysts with this property can exhibit exquisite chemoselectivity, as revealed by the Cu/nitroxyl and biomimetic quinone catalysts, or support different product formation, evident in Pd-catalyzed oxidative coupling reactions. These considerations show that the optimal overpotentials, η_{ORR} and η_{sub}, will vary for different applications. More broadly, this Perspective highlights the synergies between the fields of thermal and electrochemical catalysis and how concepts taken from one field provide a foundation for improved understanding and future opportunities in another.

AUTHOR INFORMATION

Corresponding Author

Shannon S. Stahl − Department of Chemistry, University of Wisconsin-Madison, Madison, Wisconsin 53706, United States; orcid.org/0000-0002-9000-7665; Email: stahl@chem.wisc.edu

Authors

Alexios G. Stamoulis – Department of Chemistry, University of Wisconsin−Madison, Madison, Wisconsin 53706, United States; orcid.org/0000-0003-4886-0512

David L. Bruns – Department of Chemistry, University of Wisconsin−Madison, Madison, Wisconsin 53706, United States; orcid.org/0000-0003-2455-502X

Notes

The authors declare no competing financial interest.

ACKNOWLEDGMENT

We thank Dr. James Gerken for many stimulating and insightful discussions. The content outlined incorporates results from several different research projects within our group, including those funded by the NIH NIGMS (R35 GM134929; synthetic aspects of Cu/nitroxyl, quinone, and Pd-catalyzed oxidation reactions), the U.S. Department of Energy, Office of Science, Basic Energy Sciences (DE-FG02-05ER15690; mechanistic aspects of Cu/nitroxyl-catalyzed alcohol oxidation); and the National Science Foundation (CHE-1953926, mechanistic aspects of Pd-catalyzed oxidation reactions).

REFERENCES

1. Liquid Phase Aerobic Oxidation Catalysis; Stahl, S. S., Alsters, P. L., Eds.; Wiley-VCH Verlag GmbH & Co. KGaA: Weinheim, Germany, 2016.
2. Caron, S.; Dugger, R. W.; Ruggeri, S. G.; Ragan, J. A.; Ripin, D. H. B. Large-Scale Oxidation in the Pharmaceutical Industry. *Chem. Rev.* **2006**, *106*, 2943-2989.
3. Cavani, F.; Teles, J. H. Sustainability in Catalytic Oxidation: An Alternative Approach or a Structural Evolution? *ChemSusChem* **2009**, *2*, 508-534.
4. Burns, N. Z.; Baran, P. S.; Hoffmann, R. W. Redox Economy in Organic Synthesis. *Angew. Chem. Int. Ed.* **2009**, *48*, 2854-2867.
5. Stahl, S. S. Palladium-Catalyzed Oxidation of Organic Chemicals with O_2. *Science*, **2005**, *309*, 1824-1826.
6. Solomon, E. I.; Stahl, S. S. Introduction: Oxygen Reduction and Activation in Catalysis. *Chem. Rev.* **2018**, *118*, 2299–2301.
7. Chen, W.; Huang, J.; Wei, J.; Zhou, D.; Cai, J.; He, Z-H.; Chen, Y-X. Origins of High Onset Overpotential of Oxygen Reduction Reaction at Pt-Based Electrocatalysts: A Mini Review. *Electrochemistry Communications* **2018**, *96*, 71-76.
8. Appel, A. M.; Helm, M. L. Determining the Overpotential for a Molecular Electrocatalyst. *ACS Catal.* **2014**, *4*, 630–633.
9. Pegis, M. L.; Wise, C. F.; Martin, D. J.; Mayer, J. M. Oxygen Reduction by Homogeneous Molecular Catalysts and Electrocatalysts. *Chem. Rev.* **2018**, *118*, 2340-2391.
10. Bratsch, S. G. Standard Electrode Potentials and Temperature Coefficients in Water at 298.15 K. *J. Phys. Chem. Ref. Data* 1989, 18, 1–21.
11. Nutting, J. E.; Gerken, J. B.; Stamoulis, A. G.; Bruns, D. L.; Stahl, S. S. "How Should I Think about Voltage? What is Overpotential?": Establishing and Organic Chemistry Intuition for Electrochemistry. *J. Org. Chem.* **2021**, *86*, 15875–15885.
12. Merbouth, N.; Bobbitt, J. M.; Brückner, C. Preparation of Tetramethylpiperidine-1-Oxoammonium Salts and Their

Use as Oxidants in Organic Chemistry. A Review. *Org. Prep. Proced. Int.* **2004**, *36* 1-31.
13. Nutting, J. E.; Rafiee, M.; Stahl, S. S. Tetramethylpiperidine *N*-Oxyl (TEMPO), Phthalimide *N*-Oxyl (PINO), and Related *N*-Oxyl Species: Electrochemical Properties and Their Use in Electrocatalytic Reactions. *Chem. Rev.* **2018**, *118*, 4834-4885.
14. Semmelhack, M. F.; Schmid, C. R.; Cortés, D. A.; Chou, C. S. Oxidaiton of Alcohols to Aldehydes with Oxygen and Cupric Ion, Mediated by Nitrosonium Ion. *J. Am. Chem. Soc.* **1984**, *106*, 3374-3376.
15. Bobbitt, J. M.; Brückner, C.; Merbouh, N. Oxoammonium- and Nitroxide-Catalyzed Oxidations of Alcohols. In *Organic Reactions*; Wiley: Hoboken, NJ, 2009; pp 103−424
16. Hoover, J. M.; Stahl, S. S. Highly Practical Copper(I)/TEMPO Catalyst System for Chemoselective Aerobic Oxidation of Primary Alcohols. *J. Am. Chem. Soc.* **2011**, *133*, 16901-16910.
17. Zultanski, S. L.; Zhao, J.; Stahl, S. S. Practical Synthesis of Amides via Copper/ABNO-Catalyzed Aerobic Oxidative Coupling of Alcohols and Amines. *J. Am. Chem. Soc.* **2016**, *138*, 6416-6419.
18. Rafiee, M.; Konz, Z. M.; Graaf, M. D.; Koolman, H. F.; Stahl, S. S. Electrochemical Oxidation of Alcohols and Aldehydes to Carboxylic Acids Catalyzed by 4-Acetamide-TEMPO: An Alternative to "Anelli" and "Pinnick" Oxidations. *ACS Catal.* **2018**, *8*, 6738-6744.
19. Kim, J.; Stahl, S. S. Cu/Nitroxyl-Catalyzed Aerobic Oxidation of Primary Amines into Nitriles at Room Temperature. *ACS Catal.* **2013**, *3*, 1652-1656.
20. Lambert, K. M.; Bobbitt, J. M.; Eldirany, S. A.; Wiberg, K. B.; Bailey, W. F. Facile Oxidation of Primary Amines to Nitriles Using and Oxoammonium Salt. *Org. Lett.* **2014**, *16*, 6484-6487.
21. Lennox, A. J. J.; Goes, S. L.; Webster, M. P.; Koolman, H. F.; Djuric, S. W.; Stahl, S. S. Electrochemical Aminoxyl-Mediated a-Cyanation of Secondary Piperidines for Pharmaceutical Building Block Diversification. *J. Am. Chem. Soc.* **2018**, *140*, 11227-11231.
22. Pradhan, P. P.; Bobbitt, J. M.; Bailey, W. F. Oxidative Cleavage of Benzylic and Related Ethers, Using an Oxoammonium Salt. *J. Org. Chem.* **2009**, *74*, 9524-9527.
23. Kelly, C. B.; Ovian, J. M.; Cywar, R. M.; Gosselin, T. R.; Wiles, R. J.; Leadbeater, N. E. Oxidative Cleavage of Allyl Ethers by an Oxoammonium Salt. *Org. Biomol. Chem.* **2015**, *13*, 4255-4259.
24. Richter, H.; Rohlmann, R.; García Mancheño, O. Catalyzed Selective Direct α- and γ-Alkylation of Aldehydes with Cyclic Benzyl Ethers by Using $T^+BF_4^-$ in the Presence of an Inexpensive Organic Acid or Anhydride. *Chem. Eur. J.* **2011**, *17*, 11622-11627.
25. Richter, H.; Fröhlich, R.; Daniliuc, C.-G.; García Mancheño, O. Mild Metal-Free Tandem a-Alkylation/Cyclization of *N*-Benzyl Carbamates with Simple Olefins. *Angew. Chem. Int. Ed.* **2012**, *51*, 8656-8660.
26. Anelli, P. L.; Banfi, S.; Montanari, F.; Quici, S. Oxidation of Diols with Alkali Hypochlorites Catalyzed by Oxoammonium Salts Under Two-Phase Conditions. *J. Org. Chem.* **1989**, *54*, 2970-2972.
27. Bolm, C.; Magnus, A. S.; Hildebrand, J. P. Catalytic Synthesis of Aldehydes and Ketones under Mild Conditions Using TMEPO/Oxone. *Org. Lett.* **2000,** *2*, 1173-1175.
28. De Mico, A.; Margarita, R.; Parlanti, L.; Vescovi, A.; Piancatelli, G. A Versatile and Highly selective Hypervalent Iodine (III)/2,2,6,6-Tetramethyl-1-piperidinyloxyl-Mediated Oxidation of Alcohols to Carbonyl Compounds. *J. Org. Chem.* **1997**, *62*, 6974-6977.
29. Gerken, J. B.; Pang, Y. Q.; Lauber, M. B.; Stahl, S. S. Structural Effects on the pH-Dependent Redox Properties of Organic Nitroxyls: Pourbaix Diagrams for TEMPO, ABNO, and Three TEMPO Analogs. *J. Org. Chem.* **2018**, *83*, 7323-7330.
30. Gerken, J. B.; Stahl, S. S. High-Potential Elctrocatalytic O_2 Reduction with Nitroxyl/NO_x Mediators: Implications for Fuel Cells and Aerobic Oxidation Catalysis. *ACS Cent. Sci.* **2015**, *1*, 234-243.
31. Wertz, S.; Studer, A. Nitroxide-Catalyzed Transition-Metal-Free Aerobic Oxidation Processes. *Green Chem.* **2013**, *15*, 3116-3134.
32. Cao, Q.; Dornan, L. M.; Rogan, L.; Hughes, N. L.; Muldoon, M. J. Aerobic Oxidation Catalysis with Stable Radicals. *Chem. Commun.* **2014**, *50*, 4524-4543.
33. Ryland, B. L.; Stahl, S. S. Practical Aerobic Oxidations of Alcohols and Amines with Homogeneous Copper/TMEPO and Related Catalyst Systems. *Angew. Chem. Int. Ed.* **2014**, *53*, 8824-8838.
34. Hoover, J. M.; Ryland, B. L.; Stahl, S. S. Copper/TEMPO-Catalyzed Aerobic Alcohol Oxidation: Mechanistic Assessment of Different Catalyst Systems. *ACS Catal.* **2013**, *3*, 2599-2605.
35. Hoover, J. M.; Ryland, B. L.; Stahl, S. S. Mechanism of Copper(I)/TEMPO-Catalyzed Aerobic Alcohol Oxidation. *J. Am. Chem. Soc.* **2013**, 1*35*, 2357-2367.
36. Ryland, B. L.; McCann, S. D.; Brunold, T. C.; Stahl, S. S. Mechanism of Alcohol Oxidation Mediated by Copper(II) and Nitroxyl Radicals. *J. Am. Chem. Soc.* **2014**, *136*, 12166-12173.
37. Badalyan, A.; Stahl, S. S. Cooperative Electrocatalytic Alcohol Oxidation with Electron-Proton-Transfer Mediators. *Nature* **2016**, *535*, 406-410.
38. Speelman, A. L.; Gerken, J. B.; Heins, S. P.; Wiedner, E. S.; Stahl, S. S.; Appel, A. M. Determining Overpotentials for the Oxidation of Alcohols by Molecular Electrocatalysts in Non-Aqueous Solvents. *Energy Environ. Sci.* **2022**, *15*, 4015-4024.
39. Wendlandt, A. E.; Stahl, S. S. Quinone-Catalyzed Selective Oxidation of Organic Molecules. *Angew. Chem. Int. Ed.* **2015**, *54*, 14638-14658.
40. Huynh, M. T.; Anson, C. W.; Cavell, A. C.; Stahl, S. S.; Hammes-Schiffer, A. Quinone 1 e^- and 2 e^-/2 H^+ Reduction Potentials: Identification and Analysis of Deviations from Systematic Scaling Relationships. *J. Am. Chem. Soc.* **2016**, *138*, 15903–15910.
41. Guo, A.; Zipse, H.; Mayr, H. Mechanisms of Hydride Abstractions by Quinones *J. Am Chem. Soc.* **2014**, *136,* 13863–13873.
42. Fukuzumi, S.; Ohkubo, K.; Tokuda, Y.; Suenobu, T. Hydride Transfer from 9-Substituted 10-Methyl-9,10-dihydroacridines to Hydride Acceptors via Charge-Transfer Complexes and Sequential Electron−Proton−Electron Transfer. A Negative Temperature Dependence of the Rates *J. Am Chem. Soc.* **2000**, *122,* 4286–4294.

43. Largeron, M.; Fleury, M.-B. Bioinspired Oxidation Catalysts. *Science*, **2013**, *339*, 43-44.
44. Eckert, T. S.; Bruice, T. C. Chemical Properties of Phenanthrolinequinones and the Mechanism of Amine Oxidation by *o*-Quinones of Medium Redox Potentials. *J. Am. Chem. Soc.* **1983**, *105*, 4431–4441.
45. Mure, M.; Mills, S. A.; Klinman, J. P. Catalytic Mechanism of the Topa Quinone Containing Copper Amine Oxidases. *Biochemistry* **2002**, *41*, 9269–9278.
46. Mure, M. Tyrosine-Derived Quinone Cofactors. *Acc. Chem. Res.* **2004**, *37*, 131–139.
47. Wendlandt, A. E.; Stahl, S. S. Chemoselective Organocatalytic Aerobic Oxidation of Primary Amines to Secondary Imines. *Org. Lett.* **2012**, *14*, 2850-2853.
48. Wendlandt, A. E.; Stahl, S. S. Bioinspired Aerobic Oxidation of Secondary Amines and Nitrogen Heterocycles with a Bifunctional Quinone Catalyst. *J. Am. Chem Soc.* **2014**, *136*, 506-512.
49. Wendlandt, A. E.; Stahl, S. S. Modular *o*-Quinone Catalyst System for Dehydrogenation of Tetrahydroquinolines under Amplbient Conditions. *J. Am Chem. Soc.* **2014**, *136*, 11910-11913.
50. Li, B.; Wendlandt, A. E.; Stahl, S. S. Replacement of Stoichiometric DDQ with a Low Potential o-Quinone Catalyst Enabling Aerobic Dehydrogenation of Tertiary Indolines in Pharmaceutical Intermediates. *Org. Lett.* **2019**, *21*, 1176-1181.
51. For a large-scale application, see: Merschaert, A.; Boquel, P.; Van Hoeck, J. P.; Gorissen, H.; Borghese, A.; Bonnier, B.; Mockel, A.; Napora, F. Novel Approaches Towards the LTD4/E4 Antagonist, LY290154. *Org. Process Res. Dev.* **2006**, *10*, 776−783.
52. Wang, Y.-H.; Pegis, M. L.; Mayer, J. M.; Stahl, S. S. Molecular Cobalt Catalysts for O_2 Reduction: Low-Overpotential Production of H_2O_2 and Comparison with Iron-Based Catalysts. *J. Am. Chem. Soc.* **2017**, *139*, 16458-16461.
53. Heumann, A.; Jens, K.-J.; Réglier, M. Palladium Complex Catalyzed Oxidation Reactions. *Prog. Inorg. Chem.* **1994**, *42*, 483–576.
54. Stahl, S. S. Palladium Oxidase Catalysis: Selective Oxidation of Organic Chemicals by Direct Dioxygen-Coupled Turnover. *Angew. Chem. Int. Ed.* **2004**, *43*, 3400-3420.
55. Piera, J.; Bäckvall, J.–E. Catalytic Oxidation of Organic Substrates by Molecular Oxygen and Hydrogen Peroxide by Multistep Electron Transfer—A Biomimetic Approach. *Angew. Chem. Int. Ed.* **2008**, *47*, 3506–3523.
56. Vasseur, A.; Muzart, J.; Le Bras, J. Ubiquitous Benzoquinones, Multitalented Compounds for Palladium-Catalyzed Oxidative Reactions. *Eur. J. Org. Chem.* **2015**, 4053–4069.
57. Wang, D.; Weinstein, A. B.; White, P. B.; Stahl, S. S. Ligand-Promoted Palladium-Catalyzed Aerobic Oxidation Reactions. *Chem. Rev.* **2018**, *118*, 2636-2679.
58. Liu, J.; Guðmundsson, A.; Bäckvall, J.–E. Efficient Aerobic Oxidation Molecules by Multistep Electron Transfer. *Angew. Chem. Int. Ed.* **2021**, *60*, 15686–15704.
59. Sehnal, P.; Taylor, R. J. K.; Fairlamb, I. J. S. Emergence of Palladium(IV) Chemistry in Synthesis and Catalysis. *Chem. Rev.* **2010**, *110*, 824–889.
60. *Higher Oxidation State Organopalladium and Platinum Chemistry. Topics in Organometallic Chemistry*, vol 35, Canty, A. (Ed.) Springer, Berlin, Heidelberg, 2011.
61. Hickman, A. J.; Sanford, M. S. High-valent organometallic copper and palladium in catalysis. *Nature*, **2012**, *484*, 177–185.
62. Powers, D. C.; Ritter, T. Bimetallic Redox Synergy in Oxidative Palladium Catalysis. *Acc. Chem. Res.* **2012**, *45*, 840–850.
63. He, J.; Wasa, M.; Chan, K. S. L.; Shao, Q.; Yu, J.-Q. Palladium-Catalyzed Transformations of Alkyl C–H Bonds. *Chem. Rev.* **2017**, *117*, 8754–8786.
64. Zultanski, S. L..; Stahl, S. S. Palladium-Catalyzed Aerobic Acetoxylation of Benzene Using NO_x-Based Redox Mediators. *J. Organomet. Chem.* **2015**, *793*, 263–268.
65. Inadequate thermodynamic data were available for PhOAc on the NIST WebBook to determine the free energy of formation: https://webbook.nist.gov/chemistry/ (accessed March 15, 2023).
66. Bianchi, D.; Bortolo, R.; D'Alosio, R.; Ricci, M. Biphasic Synthesis of Hydrogen Peroxide from Carbon Monoxide, Water, and Oxygen Catalyzed by Palladium Complexes with Bidentate Nitrogen Ligands. *Angew. Chem. Int. Ed.* **1999**, *38*, 706–708.
67. Stahl, S. S.; Thorman, J. L.; Nelson, R. C.; Kozee, M. A. Oxygenation of Nitrogen-Coordinated Palladium(0): Synthetic, Structural, and Mechanistic Studies and Implications for Aerobic Oxidation Catalysis. *J. Am. Chem. Soc.* **2001**, *123*, 7188–7189.
68. Konnick, M. M.; Guzei, I. A.; Stahl, S. S. Characterization of Peroxo and Hydroperoxo Intermediates in the Aerobic Oxidation of N-Heterocyclic-Carbene-Coordinated Palladium(0). *J. Am. Chem. Soc.* **2004**, *126*, 10212–10213.
69. Khusnutdinova, J. R.; Rath, P. N.; Mirica, L. M. The Aerobic Oxidation of a Pd(II) Dimethyl Complex Leads to Selective Ethane Elimination from at Pd(III) Intermediate. *J. Am. Chem. Soc.* **2012**, *134*, 2414-2422.
70. Bruns, D. L.; Musaev, D. G.; Stahl, S. Can Donor Ligands Make $Pd(OAc)_2$ a Stronger Oxidant? Access to Elusive Palladium(II) Reduction Potentials and Effects of Ancillary Ligands via Palladium(II)/Hydroquinone Redox Equilibria. *J. Am Chem. Soc.* **2020**, *142*, 19678-19688.
71. Chen, X.; Engle, K. M.; Wang, D.–H.; Yu, J.–Q. Palladium(II)-Catalyzed C–H Activation/C–C Cross-Coupling Reactions: Versatility and Practicality. *Angew. Chem. Int. Ed.* **2009**, *48*, 5094–5115.
72. Wang, D.; Izawa, Y.; Stahl, S. Rapid Pd-Catalyzed Aerobic Oxidative Coupling of Arenes: Evidence for Transmetalation between Two Pd(II)-Aryl Intermediates. *J. Am Chem. Soc.* **2014**, *136*, 9914-9917.
73. Yoneyama, T.; Crabtree, R. H. Pd(II) catalyzed acetoxylation of arenes with iodosyl acetate. *J. Mol. Cat. A* **1996**, *108*, 35–40.
74. Tisue, T.; Downs, W. J. Palladium(II)-Catalysed Nitration of Benzene. *Chem.Commun.* **1969**, *8*, 410.
75. An, Z.; Pan, X.; Liu, X.; Han, X.; Bao, X. Combined Redox Couples for Catalytic Oxidation of Methane by Dioxygen at Low Temperatures. *J. Am. Chem. Soc.* **2006**, *128*, 16028-16029.
76. Stowers, K. J.; Kubota, A.; Sanford, M. S. Nitrate as a Redox Co-Catalyst for the Aerobic Pd-Catalyzed Oxidation of Unactivated sp^3-C–H Bonds. *Chem. Sci.* **2012**, *3*, 3192-3195.

77. Zhang, W.; Lou, S.; Liu, Y.; Xu, Z. Palladium-Catalyzed Chelation-Assisted Aromatic C–H Nitration: Regiospecific Synthesis of Nitroarenes Free from the Effect of the Orientation Rules. *J. Org. Chem.* **2013**, *78*, 5932–5948.
78. Majhi, B.; Kundu, D.; Ahammed, S.; Ranu, B. C. tert-Butyl Nitrite Mediated Regiospecific Nitration of (E)-Azoarenes through Palladium-Catalyzed Directed C–H Activation. *Chem. Eur. J.* **2014**, *20*, 9862-9866.
79. Wickens, Z. K.; Guzman, P.; Grubbs, R. H. Aerobic Palladium-Catalyzed Diacetoxylation of Alkenes Enabled by Catalytic Nitrite. *Angew. Chem. Int. Ed.* **2015**, *54*, 236-240.
80. Fairlamb, I. J. S. Redox-Active NO_x Ligands in Palladium-Mediated Processes. *Angew. Chem. Int. Ed.* **2015**, *54*, 10415-10427.
81. Costas, M.; Mehn, M. P.; Jensen, M. P.; Que, L. Dioxygen Activation at Mononuclear Nonheme Iron Active Sites: Enzymes, Models, and Intermediates. *Chem. Rev.* **2004**, *104*, 939–986.
82. Huang, X.; Groves, J. T. Oxygen Activation and Radical Transformations in Heme Proteins and Metalloporphyrins. *Chem. Rev.* **2018**, *118*, 2491-2553.
83. Mukaiyama, T.; Takai, T.; Yamada, T.; Rhode, O. Nickel(II) Complex Catalyzed Epoxidation of Olefins with Molecular Oxygen and Primary Alcohol. *Chem. Lett.* **1990**, 1661-1664.
84. Yamada, T.; Takai, T.; Rhode, O.; Mukaiyama, T. Highly Efficient Method for Epoxidation of Olefins with Molecular Oxygen and Aldehydes Catalyzed by Nickel(II) Complexes. *Chem. Lett.* **1991**, *20*,1-4.
85. Weinstein, A. B.; Stahl, S. S. Palladium Catalyzed Aryl C–H Amination with O_2 via *in situ* Formation of Peroxide-Based Oxidant(s) from Dioxane. *Catal. Sci. Technol.* **2014**, *4*, 1-4.
86. Maity, A.; Hyun, S.-M.; Powers, D. C. Oxidase Catalysis via Aerobically Generated Hypervalent Iodine Intermediates. *Nat. Chem.* **2018**, *10*, 200-204.
87. Maity, A.; Hyun, S.-M.; Wortman, A. K.; Powers, D. C. Oxidation Catalysis via an Aerobically Generated Dess-Martin Periodinane Analogue. *Angew. Chem. Int. Ed.* **2018**, *57*, 7205-7209.
88. Jørgensen, K. A. Transition-Metal-Catalyzed Epoxidations. *Chem. Rev.* **1989**, *89*, 431-458.
89. Xia, Q.-H.; Ge, H.-Q.; Ye, C.-P.; Liu, Z.-M.; Su, K.-X. Advances in Homogeneous and Heterogeneous Catalytic Asymmetric Epoxidation. *Chem. Rev.* **2005**, *105*, 1603-1662.
90. Takai, T.; Hata, E.; Yamada, T.; Mukaiyama, T. *Bull. Chem. Soc. Jpn.* **1991**, *64*, 2513-2518
91. Qi, J.-Y.; Li, Y.-M.; Zhou, Z.-Y.; Che, C.-M.; Yeung, C.-H.; Chan, A. S. C. Novel Manganese Complex as an Efficient Catalyst for the Isobutyraldehyde-Mediated Epoxidation of Cyclic Alkenes with Dioxygen. *Adv. Synth. Catal.* **2005**, *347*, 45–49.
92. Wentzel, B. B.; Alsters, P. L.; Feiters, M. C.; Nolte, R. J. M. Mechanistic Studies on the Mukaiyama Epoxidation. *J. Org. Chem.* **2004**, *69*, 3453-3464.
93. Lassila, K. R.; Waller, F. J.; Werkheiser, S. E.; Wressell, A. L. Aldehyde/olefin cooxidations: Parallel epoxidation pathways and concerted decomposition of the peroxyacyl-olefin adduct. *Tetrahedron Lett.* **1994**, *35*, 8077–8080.
94. Vreugdenhil, A. D.; Reit, H. Liquid-phase CO-oxidation of aldehydes and olefins radical versus non-radical epoxidation. *Recl. Trav. Chim. Pays-Bas* **1972**, *91*, 237–245.
95. Tsuchiya, F.; Ikawa, T. Liquid-phase oxidation of 2-butene in the presence of benzaldehyde. *Can. J. Chem.* **1969**, *47*, 3191–3197.
96. Bartlett, P. D. Recent Work on the Mechanisms of Peroxide Reactions. *Rec. Chem. Prog.* **1950**, *11*, 47.
97. Singleton, D. A.; Merrigan, S. R.; Liu, J.; Houk, K. N. Experimental Geometry of the Epoxidation Transition State. *J. Am. Chem. Soc.* **1997**, *119*, 3385–3386.
98. Sommovigo, M.; Alper, H. Aerobic oxidation of ethers and alkenes catalyzed by a novel palladium complex. *J. Mol. Catal.* **1994,** *88*, 151–158.
99. Cornell, C. N.; Sigman, M. S. Discovery of and Mechanistic Insight into a Ligand-Modulated Palladium-Catalyzed Wacker Oxidation of Styrenes Using TBHP. *J. Am. Chem. Soc.* **2005**, *127*, 2796–2797.
100. Yan, Y.; Feng, P.; Zheng, Q.-Z.; Liang, Y.-F.; Lu, J.-F.; Cui, Y.; Jiao, N. $PdCl_2$ and N-Hydroxyphthalimide Co-catalyzed C_{sp2}–H Hydroxylation by Dioxygen Activation. *Angew. Chem. Int. Ed.* **2013**, *52*, 5827–5831.
101. Zhuang, Z.; Yu, J.-Q. Lactonization as a general route to β-C(sp^3)–H functionalization. *Nature* **2020**, *577*, 656–659.
102. Zhdankin, V. V.; Stang, P. J. Chemistry of Polyvalent Iodine. *Chem. Rev.* **2008**, *108*, 5299-5358.
103. Radzhabov, M. R.; Sheremetev, A. B.; Pivina, T. S. Oxidative ability of organic iodine(III) reagents: a theoretical assessment. *New J. Chem.*, **2020**, *44*, 7051-7057.
104. Lide, D. R. ed. (2006). CRC Handbook of Chemistry and Physics (87th ed.). Boca Raton, FL: CRC Press. ISBN 0-8493-0487-3.
105. Hyun, S.-M.; Yuan, M.; Maity, A.; Gutierrez, O.; Powers, D. C. The Role of Iodanyl Radicals as Critical Chain Carriers in Aerobic Hypervalent Iodine Chemistry. *Chem.* **2019**, *5*, 2388-2404.

TOC graphic

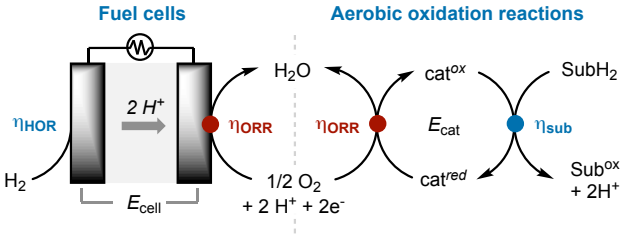
Fuel cells
Aerobic oxidation reactions
2 H+
ηHOR
ηORR
H2
Ecell
H2O
1/2 O2
+ 2 H+ + 2e-
ηORR
catox
catred
Ecat
ηsub
SubH2
Subox
+ 2H+